

# A method for laser rangefinder reticle position calibration in a multi-sensor imaging system

Saša Vujić, *Member, IEEE*, Miloš Radisavljević, *Member, IEEE*, Dragana Perić, *Senior Member, IEEE* and Branko Livada, *Senior Member, IEEE*

**Abstract**— A method for laser rangefinder reticle position calibration in a multi-sensor imaging system is presented. This method was developed to provide system control software with proper parameters used for LRF reticle position, for all imagers and for different field of view configurations of those imagers in a typical multi-sensor imaging system. The importance of reticle position calibration and accuracy is explained, and error calculated. A prerequisite for laser rangefinder reticle position calibration is to perform each imager calibration and the multi-sensor imaging system optical axes rectification. The method is straight forward, fast and reliable. Details of the method are described and experimental verification of results obtained after the calibration are given.

**Index Terms**—laser rangefinder; LRF; reticle calibration; multi-sensor imaging system; electro-optical system; long-range surveillance.

## I. INTRODUCTION

Multi-sensor imaging systems (MSIS) with zoom lenses are used for surveillance with number of technical, technological and application challenges [1], and also for other applications where observed object of interest (target) distance is important, e.g. target geolocation. These MSIS' functionalities are related with the use of laser rangefinders (LRF) and their proper integration within the MSIS [2], [3]. A control station – operator's console, which provides a user interface to MSIS sensors data, is another important part of MSIS [4]. In order to create a usable system it is necessary to provide a system operator with possibility to accurately point with LRF beam to desired object of interest. For this purpose it is necessary to determine control software parameters used for LRF reticle positioning. With properly determined parameters control software displays the LRF reticle at the right place and operator is able to direct the MSIS, i.e. the LRF beam to target, for any selected field of view (FOV).

Saša Vujić is with the Vlatacom Institute of High Technologies, 5 Milutina Milankovića Blvd., 11070 Belgrade, Serbia (e-mail: [sasa.vujic@vlatacom.com](mailto:sasa.vujic@vlatacom.com)), and with the Belgrade Metropolitan University, Tadeuša Košćuška 63, 11000 Beograd, Serbia

Miloš Radisavljević is with the Vlatacom Institute of High Technologies, 5 Milutina Milankovića Blvd., 11070 Belgrade, Serbia (e-mail: [milos.radisavljevic@vlatacom.com](mailto:milos.radisavljevic@vlatacom.com)), and with the Belgrade Metropolitan University, Tadeuša Košćuška 63, 11000 Beograd, Serbia

Dragana Perić is with the Vlatacom Institute of High Technologies, 5 Milutina Milankovića Blvd., 11070 Belgrade, Serbia (e-mail: [dragana.peric@vlatacom.com](mailto:dragana.peric@vlatacom.com)).

Branko Livada is with the Vlatacom Institute of High Technologies, 5 Milutina Milankovića Blvd., 11070 Belgrade, Serbia (e-mail: [branko.livada@vlatacom.com](mailto:branko.livada@vlatacom.com)).

This work is continuation of work published in [2] and [3], where LRF integration, LRF reticle integration and camera calibration are described. In available literature there are also other articles related to these topics [5-12], however, the details and methods about how to determine control software parameters used for LRF reticle positioning are not readily available, and therefore we are not able to make any comparison with other calibration methods in the sense of complexity and accuracy.

In this work the main research issue was to establish the correlation between LRF beam, images from different imagers and for any FOV, and reticle which is shown on display. Furthermore, the particular goal was to define a method for determining control software parameters used for LRF reticle position.

In this paper in section II we describe a typical electro-optical MSIS architecture and basic functionalities, in section III some zoom lens properties, in section IV we explain the importance of LRF reticle position calibration and its accuracy, in section V we list prerequisites for LRF reticle calibration, in section VI we present a method for LRF reticle position calibration in a multi-sensor imaging system, in section VII we summarize results of the method experimental verification, and in section VIII we give the conclusion.

## II. ELECTRO-OPTICAL MULTI-SENSOR SYSTEM ARCHITECTURE AND BASIC FUNCTIONALITIES

Multi-sensor imaging systems (MSIS) are used for surveillance, observed object geolocation and other applications [13], [14]. Each of those systems comprises an electro-optical head with integrated sensors mounted on a gimbal, and remote operator's console with application software for monitoring and control [4].

A typical MSIS with MWIR thermal imager, visible light imager and a LRF mounted on a gimbal is shown in Fig. 1.



Fig. 1. Multi-sensor imaging systems with laser rangefinder.

The sensors that those systems usually comprise [1] are

midwave infrared (MWIR) or longwave infrared (LWIR) thermal imagers with continuous zoom optics, visible light imagers with continuous zoom optics, short-wave infrared (SWIR) imagers with continuous zoom optics, laser rangefinders (LRF), positioning sensors and orientation sensors. Such systems are capable of measuring the line of sight distance from the electro-optical head with sensors to some object of interest, by using a LRF, and are also capable to accomplish many other more advanced tasks, e.g. calculating observed object of interest geolocation, based on known data about MSIS position, orientation and observed object distance [15-17].

A MSIS operator uses such a system through an operator's console with input and output devices, via a graphical user interface (GUI) which is a part of a software application for monitoring and control installed on the operator's console [4]. The operator's console can be in different forms, with one or more displays as output device, and with joystick, touchpad, trackball, touchscreen, keyboard or mouse as input device. An example of operator's console is shown in Fig. 2.



Fig. 2. Multi-sensor imaging system operator's console with three displays.

The GUI provides video streams for each of the integrated imagers, as well as other data, statuses and controls for MSIS functionalities. Depending on the selected operator's console for the particular application, the GUI is usually optimized to provide the best possible usability in a given scenario. An example of GUI with two video streams, map, statuses and controls is shown in Fig. 3.

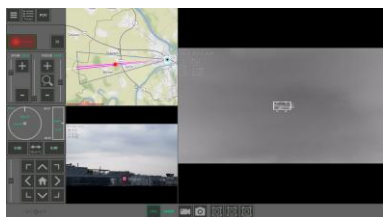


Fig. 3. Graphical user interface (GUI) of an operator's console, with two video streams, map, statuses and controls.

For each of the video streams there is an option to display a LRF reticle which shows the operator where the LRF beam is aiming. A video stream with reticle is shown in Fig. 4.

In order to bring such a system into the function there is a need to perform calibrations on different levels, including the continuous zoom imagers' calibration. One of the calibration tasks is to perform a calibration of LRF reticle position coordinates, for each imager, for different zoom levels. Before performing this reticle position calibration it is necessary to perform optical axes alignment to set up the axes of all

imagers and LRF to be parallel to each other (a process called optical axes rectification, or boresighting).

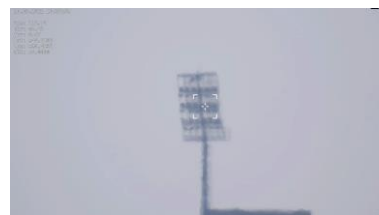


Fig. 4. Video stream with LRF reticle (object distance 4320m).

The optical axes rectification process is performed by means of precise mechanical positioning of structures holding optical elements. The optical axis rectification process is performed with zoom optics set in high end position, which gives a narrow field of view (NFOV), in order to achieve better accuracy. However, other fields of view (FOV) are also of interest and in order to provide a proper alignment of reticle for different zoom levels (different FOVs) there is a need to calibrate reticle position for different zoom levels due to an inherent characteristic of zoom lens to have deviation of optical axis from the ideal one when changing the zoom level. Therefore, the process of optical axis rectification does not have to be perfect and several pixels displacement can be allowed. Those displacements can be compensated by means of precision positioning of reticle in the image, i.e. in each frame of the video streams. The size of the reticle corresponds to the solid angle of the LRF beam. A typical LRF reticle, as drawn on visible light imager is shown in Fig. 5.



Fig. 5. LRF reticle as shown on screen

The process of reticle position coordinates calculation for all imagers and for different FOVs is time consuming and requires highly skilled operators and their high concentration, with high risk of making mistakes during the process. Therefore, in Vlatacom Institute we developed a method for LRF reticle position calibration such that the whole process is straight forward, fast and not prone to random errors.

### III. ZOOM LENS PROPERTIES

Zoom lenses are very popular in modern multi-sensor imaging systems used in long-range surveillance and related applications. They provide flexibility and controllability for different missions and use cases. Zoom lenses provide users with a functionality to observe areas with any FOV angle, from a wide field of view (WFOV) to NFOV, and also to focus objects on different distances from minimal object distance (MOD), to infinite distance, for any FOV. Some of

the basic properties of each zoom lens are minimal and maximal focal length -  $f_{min}$  and  $f_{max}$ , f-number - N, WFOV, NFOV and MOD. There are also many others which define lens optical characteristics and electro-mechanical interfacing.

WFOV and NFOV of imager depend on imaging sensor size and minimal/maximal lens focal lengths. WFOV, NFOV of two MSIS, C330 and C1000, are given in Table I.

TABLE I  
CONTINUOUS ZOOM LENS PARAMETERS OF TWO THERMAL AND TWO VISIBLE LIGHT IMAGERS

Lens\Par.	WFOV [°]	NFOV [°]	$f_{min}$ [mm]	$f_{max}$ [mm]
C330-VIS	36	3.5	16	160
C330-TH	35.4	1.67	16	330
C1000-VIS	21	0.55	20	800
C1000-TH	18	0.75	40	1000

The thermal imager resolution is 640 x 480 with pixel size of 15  $\mu$ m for C330-TH, and 1280 x 1024 with pixel size of 10  $\mu$ m for C1000-TH.

One of the important properties is back focal length (BFL), also known as flange focal distance (FFD), flange focal depth (FFD), flange back distance (FBD), flange focal length (FFL). BFL defines the position of the zoom lens focal plane distance, where the imaging sensor plane should be placed, and the lens mounting reference plane. The adequate distance of the imaging sensor will result in the a possibility to focus objects from MOD to infinite distance, for any FOV from WFOV to NFOV. A typical test target used for back focus calibration, USAF 1951, is show in Fig. 6.

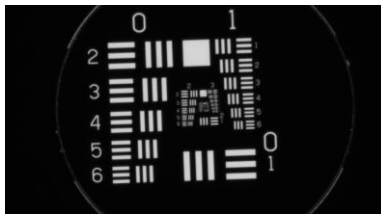


Fig. 6. USAF 1951 test target used for back focus calibration.

The zoom lens functionality is based on moving mechanisms which inherently involve lens elements displacements relatively to their ideal positions. For this reason it is necessary to perform additional zoom lens calibration for proper alignment of LRF reticle with LRF beam [17-21].

All these calibrations are necessary for successful LRF integration in any MSIS [2], [3].

Instantaneous field of view or (IFOV) is an important parameter which determines how much a single pixel can see in terms of FOV, depends on pixel size and focal length and equals  $IFOV = \text{Pixel Size} / \text{Focal Length}$ . With zoom lenses IFOV changes with FOV from wide IFOV( $f_{min}$ ) to narrow IFOV( $f_{max}$ ) angle.

#### IV. THE IMPORTANCE OF RETICLE CALIBRATION AND ITS ACCURACY

The LRF beam is quite narrow with Gaussian distribution [2] and in tested systems it is circular in shape with divergence angle of 700  $\mu$ rad in case of MSIS C330, and 250  $\mu$ rad in case of MSIS C1000. Both are eye safe with 1,54  $\mu$ m wavelength. The maximal measurement ranges are 20 km and 39 km, with range measurement accuracy of  $\pm 5$  m, and  $\pm 1$  m respectively. The minimal IFOV (at NFOV) in tested systems is 32  $\mu$ rad in case of MSIS C330, and 5  $\mu$ rad in case of MSIS C1000. For these cases the LRF beam divergence is 22 to 50 pixels.

If the LRF reticle was not well aligned with the LRF beam the LRF functionality would be lost, due to the fact that LRF beam would miss the target, i.e. it would not hit the area where the MSIS operator is targeting with the reticle, resulting in a wrong measured data, or no measurement at all. If the reticle was quite well aligned with the beam, but not perfectly, it would be possible to measure the object distance, but for any mistake or deviation in misalignment between the reticle and LRF beam an added error in geolocation calculation [16] would be made. With MSIS C330, at 10 km distance, the error introduced with reticle misalignment is 0,32 m for each pixel of reticle displacement. Therefore, the accuracy of reticle positioning is important for such systems. In a simplified model of MSIS, the LRF beam is an ideal line corresponding to the center of the reticle shown on the screen. However, in real case the center of LRF beam will not match ideally to the reticle center, as shown in Fig. 7.

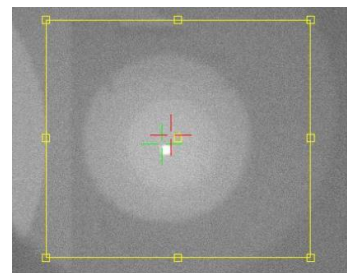


Fig. 7 Displacement of reticle and LRF

For some real MSIS and long distances at which these systems are used, the error that is made due to the reticle displacement can be significant. The error in geolocation calculation for one pixel of reticle displacement on real systems for four different imagers given in Table I, at distances of 1, 2, 5, 8 and 10 km, are given in Table II.

TABLE II  
ERROR IN GEOLOCATION CALCULATION FOR ONE PIXEL OF RETICLE DISPLACEMENT AT DISTANCES OF 1, 2, 5, 8 AND 10 KM, IN MM

Error in mm	Distance				
	1km	2km	5km	8km	10km
C330-VIS	32	64	159	255	318
C330-TH	46	91	228	364	455
C1000-VIS	5	10	25	40	50
C1000-TH	10	20	51	82	102

The error in geolocation calculation at object distance of 10 km, for 1, 2, 5, 8 and 10 pixels of reticle displacement on real systems for four different imagers given in Table I, are given in Table III.

TABLE III  
ERROR IN GEOLOCATION CALCULATION AT 10KM DISTANCE FOR RETICLE DISPLACEMENTS OF 1, 2, 5, 8 AND 10 PIXELS, IN M

Error in m	Displacement				
	1 px	2 px	5 px	8 px	10 px
Imager					
C330-VIS	0,32	0,64	1,59	2,54	3,18
C330-TH	0,46	0,91	2,28	3,64	4,55
C1000-VIS	0,05	0,10	0,25	0,40	0,50
C1000-TH	0,10	0,20	0,51	0,82	1,02

V. THE PREREQUISITES FOR LRF RETICLE CALIBRATION

A prerequisite for LRF reticle calibration is to perform each imager “zoom to FOV” calibration [2]. Depending on non-linearity of imager lens characteristic it is necessary to decide the number and value of discrete zoom lens positions for which the reticle will be calibrated. For all other zoom lens positions, in between the selected discrete positions, the reticle position will be calculated during the run time in the software application, using piecewise-linear approximation.

Furthermore, it is necessary to perform MSIS optical axes rectification, by means of precise mechanical positioning of structures holding optical elements, which is usually performed in NFOV setup for each imager. This way we will ensure that the calibrated MSIS will have the full correspondence of each imager reticle presenting the area where the LRF beam is aiming. In the ideal case the beam central line will correspond to each reticle central point. When the optical axes are nearly parallel, which can be observed and confirmed with use of collimator (few pixels displacement can be tolerated), a procedure of LRF reticle position calibration can be started.

It is necessary to perform the described procedure for each of the imagers contained in the MSIS. The sequence of the imagers’ reticle calibration is irrelevant. Therefore the procedure can be started with any of the imagers that are contained in the MSIS. A MSIS set up in front of the collimator for rectification of visible light imager with LRF is presented in Fig. 8.



Fig. 8 A MSIS set up for rectification of visible light imager in front of the collimator

If the LRF is equipped with properly aligned visible light boresighting LED source, it can be used to make LRF reticle calibration, instead of LRF emitter. In that case instead of capturing videos a single image can be captured for each FOV. The same method can be used for LRF devices that can operate in continuous measurement mode (CMM). A single image will be sufficient for determining of LRF beam central point.

VI. A METHOD FOR LRF RETICLE POSITION CALIBRATION IN A MULTI-SENSOR IMAGING SYSTEM

Within this method there are four stages to be completed. In the first stage the raw data should be captured, then in the second stage the position of LRF beam in the target should be determined, for each FOV. In the third stage the reticle calibration parameters should be calculated, and finally in the fourth stage the calibration parameters should be entered into software application that draws the reticle in the video stream.

For the first stage we need a device under test (DUT), in this case a selected imager, and an appropriate collimator for the selected imager’s maximal focal length. In Fig. 9 an image taken with visible light imager of LRF firing in a target is shown.

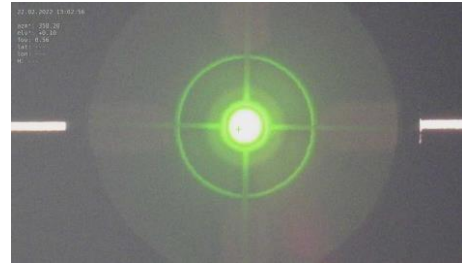


Fig. 9. Image taken with visible light imager of LRF firing in a target

All steps of the first stage are shown in block diagram in Fig. 10.

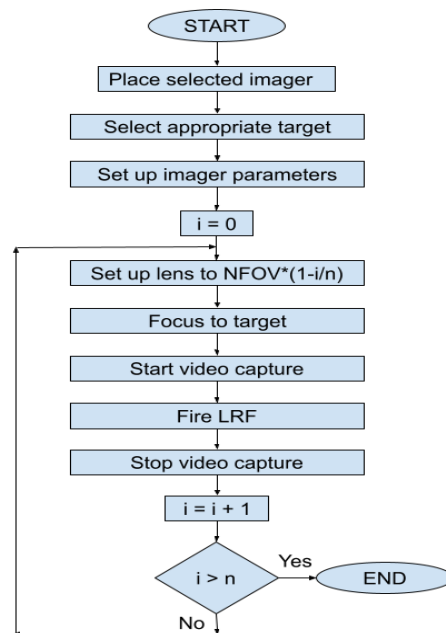


Fig. 10. Block diagram for first stage of the LRF calibration



The procedure is then repeated for each of the imagers contained in the MSIS.

When all videos are captured, for all imagers, then the first stage of this process is finished and the second stage can start. In the second stage for each captured video from the first stage we extract a frame in which the LRF beam is clearly visible. From that frame we determine the central coordinates of the LRF beam relatively to the image center.

In Fig. 11 an image taken with visible light imager of LRF firing in a target is shown.



Fig. 11. Image taken with thermal imager of LRF firing in a target

For small angles close to NFOV the displacement from the image central coordinates to the LRF beam central coordinates depend on precision of optical axes rectification performed in previous stage. For wider angles closer to WFOV the displacement of LRF beam central coordinates depend on lens' construction. That can be seen also on the Fig. 12 where the reticle displacement in pixels for visible light and thermal imager are shown, for x and y axes. In case of visible imager the displacements are in range from 0 to 29 pixels in x axis, and from -6 to 29 pixels in y axis. In case of thermal imager the displacements are in range from -7 to 4 pixels in x axis, and from -1 to -12 pixels in y axis. In this case the displacements are higher for visible light imager due to the fact that its IFOV is twice smaller then in thermal imager.

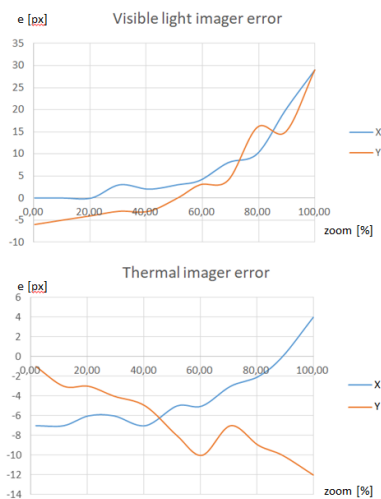


Fig. 12. Reticle displacement in pixels for visible light and thermal imager

When we have central coordinates for all imagers for each selected FOV, then in stage three we calculate reticle

positioning parameters. As a result we have x and y reticle positioning parameters for each imager.

Finally, in stage four, the reticle positioning parameters can be entered into the software application that draws the reticle in the video stream.

By default, without the calibration, the reticle is drawn in the center of the video stream for any FOV. Only after the calibration parameters are entered the reticle will be drawn displaced to the image center, corresponding to the relative displacement of the LRF beam for any selected FOV.

VII. RESULTS OF EXPERIMENTAL VERIFICATION

The proposed method for LRF reticle position calibration has been verified in real conditions using available MSIS. The MSIS has been placed on the rooftop of the building from where there is a good view on existing remote objects.



Fig. 13. A heating plant chimney at 8km distance used to verify the x-axis deviations of the reticle, in thermal and visible imager

The most appropriate objects for verification of LRF beam correspondence with reticle position on the screen are those objects which have large and sharp edges. It is important to use remote objects on relatively long distances, in order to minimize error due to non-coaxial quasi parallel axes of

imagers and LRF.

In this particular case a heating plant chimney at 8km distance was used to verify the x-axis deviations of the reticle from the ideal case in NFOV. Images taken with thermal and visible light imagers are shown in Fig. 13.

For verification of y-axis a rooftop heliport structure with upper and lower limits, at the distance of 620m was used as shown in Fig. 14.



Fig. 14. A rooftop heliport structure with upper and lower limits, at the 620m distance, used to verify the y-axis

Several LRF measurements have been accomplished in order to confirm where the LRF beam is really aiming and to verify the good correspondence with the LRF reticle on the screen. It has been shown that deviation is equal to 2 pixels in thermal imager, which in this case corresponds to 0.1 mrad, and 3 pixels in color imager, which in this case corresponds to 0.15 mrad.

Furthermore, it has been shown that for other FOVs reticle deviation from the ideal one is similar in pixel size, but is lower in angle, due to larger FOV angles.

### VIII. CONCLUSION

The described method was implemented to provide straight forward, fast and reliable process of reticle position calibration. The calibration process is complex but with this method it is straight forward, and can be performed by trained personnel. It is fast allowing efficient use of expensive equipment. Furthermore, it is reliable resulting in high process efficiency. However, there is a need for further work on additional improvements in process of reticle calibration. The further work will focus on automatic extraction of LRF spot central coordinates based on image processing techniques which can be applied on the same images taken during the reticle calibration process.

### ACKNOWLEDGMENT

Authors would like to thank Vlatacom Institute for equipment and support which enabled continuous work and

improvements in the field of electro-optics. This work was undertaken within the Vlatacom Institute project P157.

### REFERENCES

- [1] D. Perić, B. Livada, „Technical, technological and application limitations of the electro-optical surveillance systems“, 8th International Conference on Defensive Technologies, OTEH 2018, Belgrade, Serbia, 11-12 October 2018
- [2] B. Livada, D. Perić, M. Perić, „Challenges of Laser Range Finder Integration In Electro-Optical Surveillance System“, 4th International Conference on Electrical, Electronic and Computing Engineering IcETRAN 2017, Kladovo, Serbia, June 05 – 08, 2017
- [3] B. Tomić, D. Perić, M. Radisavljević, S. Vujić, „Reticle Integration and Camera Calibration in Multi Sensor Surveillance Systems“, 8th International Conference on Defensive Technologies, OTEH 2018, Belgrade, Serbia, 11-12 October 2018
- [4] D. Perić, S. Vujić, B. Livada, „Multi-sensor system operator’s console: Towards structural and functional optimization“, 7th International Conference on Defensive Technologies, OTEH 2016, Belgrade, Serbia, 6-7 October 2016
- [5] S. M. Ayaz, M. Y. Kim, J. Park, Survey on zoom-lens calibration methods and techniques”, *Machine Vision and Applications*, July 2017
- [6] A. Pennisi, D. Bloisi, C. Gaz, L. Iocchi, D. Nardi, “Novel Patterns and Methods for Zooming Camera Calibration”, *Journal of WSCG*, Volume 21, Number 1, 2013, pp. 59-67
- [7] Z. Wu, and R. J. Radke, “Keeping a Pan-Tilt-Zoom Camera Calibrated”, *IEEE Transactions on Pattern Analysis and Machine Intelligence*, November 2012
- [8] S. Upadhyay, S.K.Singh, M. Gupta, A. K. Nagawat, “Linear and Non-linear Camera Calibration Techniques”, *Journal of Global Research in Computer Science*, Volume 2, No. 5, April 2011
- [9] B. Wu, H. Hu, Q. Zhu, and Y. Zhang, “A Flexible Method for Zoom Lens Calibration and Modeling Using a Planar Checkerboard”, *Photogrammetric Engineering & Remote Sensing*, Vol. 79, No. 6, June 2013, pp. 555–571
- [10] Z. Wang, J. Mills, W. Xiao, R. Huang, S. Zheng and Z. Li, “A Flexible, Generic Photogrammetric Approach to Zoom Lens Calibration”, *Remote Sens.* 2017, 9, 244
- [11] S. Zheng, Z. Wang, R. Huang, “Zoom lens calibration with zoom- and focus-related intrinsic parameters applied to bundle adjustment”, *ISPRS Journal of Photogrammetry and Remote Sensing* 102 (2015), pp. 62–72
- [12] Reg G. Willson, S. A. Shafer, “What is the center of the image?”, *J. Opt. Soc. Am. A* / Vol. 11, No. 11/, November 1994
- [13] J. Y. Dufour (Editor), *Intelligent Video Surveillance Systems*. ISTE Ltd. London and John Wiley & Sons Inc., New York, 2013
- [14] A. K. Maini, *Lasers and Optoelectronics: Fundamentals, devices and applications*, John Wiley and Sons, Chichester, UK, 2013
- [15] J. A. Ross, B. R. Geiger, G. L. Sinsley, J. F. Horn, L. N. Long, and A. F. Niessner: “Vision-Based Target Geolocation and Optimal Surveillance on an Unmanned Aerial Vehicle”, *AIAA Paper 2008-7448*, *AIAA Guidance Navigation and Control Conference*, Honolulu, Hawaii, 2008
- [16] Livada, B.; Vujić, S.; Radić, D.; Unkašević, T.; Banjac, Z. Digital Magnetic Compass Integration with Stationary, Land-Based Electro-Optical Multi-Sensor Surveillance System. *Sensors* 2019, 19, 4331. <https://doi.org/10.3390/s19194331>
- [17] B. Livada, S. Vujić, „Target position CEP50 estimation using electro-optical multisensory surveillance system“, 8th International Conference on Defensive Technologies, OTEH 2018, Belgrade, Serbia, 11-12 October 2018
- [18] D.C. Dilworth, “A zoom lens from scratch: the case for number crunching”, *Proc. SPIE 9947, Current Developments in Lens Design and Optical Engineering XVII*, 994702 (27 September 2016)
- [19] R. N. Youngworth and E. I. Betensky, “Fundamental Consideration for zoom lens Design (tutorial)”, *Proc. SPIE*, Vol. 8488, *Zoom Lenses IV*, 2012
- [20] Rowlands, D. Andrew, *Field guide to photographic science*, SPIE Press, Bellingham, USA, 2020
- [21] S. Zhou and L. Jiang: ”A modern description of Rayleigh’s criterion“, *Phys. Rev. A* , 99, 013808, 2019.